

FILE COPY
NO. 2

FILE COPY
NO. 1-W

CASE FILE COPY

TECHNICAL MEMORANDUMS

NATIONAL ADVISORY COMMITTEE FOR AERONAUTICS

No. 477

CONTRIBUTION TO THE DESIGN AND CALCULATION OF
FUEL CAMS AND FUEL VALVES FOR DIESEL ENGINES

By Jatindra Nath Basu

From Der Motorwagen, May 10 and July 31, 1927

Washington
August, 1928

FILE COPY

To be returned to
the files of the National
Advisory Committee
for Aeronautics
Washington, D. C.

NATIONAL ADVISORY COMMITTEE FOR AERONAUTICS.

TECHNICAL MEMORANDUM NO. 477.

CONTRIBUTION TO THE DESIGN AND CALCULATION OF
FUEL CAMS AND FUEL VALVES FOR DIESEL ENGINES.*

By Jatindra Nath Basu.

Diesel-engine builders have always experienced great difficulties in adjusting the engines. This was largely due to the unsuitable course of the lift of the fuel-valve needle which was, in turn, due to the poor shape of the fuel cam. Before placing a new engine in operation, some simple form of cam (as shown, e.g., by Fig. 1) was first adopted for the fuel injection. This cam had to be filed into the correct shape with the aid of the indicator diagrams, whereby the best shape of the nozzle (Figs. 2-4) was still unknown. This harmonizing of the cam and indicator diagram was an expensive and tedious task, which might last a week or more, before obtaining a good diagram with good combustion. Although considerable progress has been made and many data have been collected, no scientific investigation of the shape of the cam and its effect on the indicator diagram, on the combustion and on the functioning of the engine has yet been made.

In this work I have attempted to find a basis for the design of fuel cams, which will serve equally for large and small engines, both high-speed and low-speed. A cam must serve:

*"Beitrage zum Entwurf und zur Berechnung der Brennstoffnocken und Brennstoffventile von Dieselmotoren," from Der Motorwagen, May 10 and July 31, 1927.

1. To obtain a good uniform pressure diagram from the engine at various loads;
2. To produce an efficient, smokeless combustion of the fuel;
3. To enable the smoothest and quietest possible functioning of the fuel valve.

These purposes must also be served within the required range of overloading.

It is already known that the size of an engine and its revolution speed greatly affect its fuel combustion and its quietness of functioning. It is obvious that the correct shape of the cam depends largely on the size and revolution speed of the engine. It is therefore no easy task to find a common basis for the cams of all engines, large and small, high-speed and low-speed. We must clearly understand that even a well-built and well-installed engine is useless if it does not run smoothly. It is hard to realize the great influence of the valve-lift curve on the combustion and on the indicator diagram. A well-made injection valve cannot always prevent poor combustion, though a rightly shaped cam can very easily improve it. In shaping a cam, an accuracy of 0.01 mm (0.0004 in.) is required and is, in fact, attained. Good workshops have devices which, at various crank angles, render it possible to measure the valve lift accurately to within 0.01 mm (0.0004 in.) and to estimate

it to within 0.001 mm (0.00004 in.).

I have also attempted to determine the various cross sections which occur in a fuel valve of a Diesel engine, and the most important dimensions which can serve as a basis for the design.

Tested Types of Injection Valves

For my experiments I selected two widely used, typical valves. Moreover, one of these valves is used in large engines and the other in small engines.

1. Sleeve valves.— Figure 2 shows an injection valve containing a sleeve atomizer suitable for small cylinders, of $D = 310$ mm (12.2 in.), $H = 350$ mm (13.78 in.), $n = 400$ R.P.M. At various points (A, a_1 , a, b to g) I have calculated the cross sections, through which the injection air and the fuel must flow before reaching the combustion space in the cylinder. These cross sections are represented in Figure 3. The need of such a tower-shaped series of cross sections, during the atomization and flow of the mixture of fuel and air, cannot yet be proved, but it is obvious that turbulence is produced by this form of cross section.

2. Disk valves.— Figure 4 shows an injection valve with a disk atomizer. This is used in engines of 400-500 HP. per cylinder, with $D = 740$ mm (29.13 in.), $H = 1200$ mm (47.24 in.), $n = 125$ R.P.M. Figure 5 shows the course of the cross sections

during the atomization and flow. It is also a tower-shaped diagram. The cross sections at the various points A, a_1 , a, b, etc., are given in the following table for both kinds of valves.

Fuel valve with	Cross sections in mm at the points										
	A	a_1	a	b	c	d	e	At maximum needle lift		f	g
								h	x		
Sleeve atomizer	174	302	43.2	117 105	70 111	97.5 44.1	38 97	Max. 33.4	of 2.5 15.4	28.3 95	15.14
Disk atomizer	1402	1882	1560	339	1882	225	225 488	Max. 137	of 4.0 70.4	201	62.8

Shape of Fuel Cam and Its Effect on the Indicator Diagram

The fuel-valve cam is one of the most important parts of a Diesel engine, which fact is hardly obvious from a superficial consideration of the engine. If the cam is not shaped rightly, days of wearisome work are required to produce a fairly good indicator diagram combined with good combustion and quiet functioning. If the shape of the cam is very bad, good execution avails nothing. Experimentation is advisable in order to enable a thorough investigation of the effect of the cam shape on the indicator diagram and to avoid needless waste of time and money. The following investigations are based on such experimentation. It was initiated with cam No. 1 (Fig. 6), which is well-known from previous experiments. Figure 7 shows the various points a, b, c, d of cam No. 1, and the following table gives the needle lift at various crank angles for each position of the cam.

Cam No. 1

Position a		b		c		d	
Crank angle	Needle lift mm	Crank angle	Needle lift mm	Crank angle	Needle lift mm	Crank angle	Needle lift mm
-6°	0	-5°	0	-4°	0	-3°	0
-3°	0.25	-2°	0.25	-2°	0.15	-3°	0
Dead center}	0.6	0T	0.46	0T	0.34	0T	0.2
+5°	1.45	+5°	1.22	+5°	1.02	+5°	0.82
10°	2.3	10°	2.13	10°	1.99	10°	1.78
15°	2.6	15°	2.6	15°	2.6	15°	2.52
20°	2.25	20°	2.4	20°	2.48	20°	2.54
25°	1.38	25°	1.52	25°	1.75	25°	1.82
30°	0.37	30°	0.55	30°	0.70	30°	0.9
35°	0	35°	0	35°	0.05	35°	0.12
	-	36°	-	37°	0	38°	0

The minus sign means "before the dead center" and the plus sign means "after the dead center."

Corresponding to each position (a, b, c and d) of the cam, the indicator diagrams 1, 2, 3 and 4 in Figure 9 were obtained. The diagrams are all pointed and show a combination of the constant-pressure and constant-volume principles, somewhat as found in compressorless engines. The final compression pressure was 29 atg (atmosphere gauge pressure) and the injection pressure was 57 atg in all cases. There should be noted:

1. The maximum combustion pressure;
2. The width of the diagram measured on a horizontal line passing through the final compression pressure of 29 atg, as shown in Figure 9. The dependence of the final combustion pressure and of the width of the diagram at the beginning of the injection was measured for the cam positions a, b, c and d and

recorded in the following table.

Crank angle of injection before dead center	Maximum combustion pressure	Width of indicator diagram
6°	40 atg	3.0 mm
5°	37 "	3.5 "
4°	35 "	3.8 "
3°	34 "	4.5 "

From the above data it is apparent that the maximum pressure increases and the diagram grows narrower as the beginning of the injection is advanced.

Indicator diagram No. 4 (Fig. 9) shows the typical characteristics of retarded combustion. The combustion had not yet started at the beginning of the working stroke, and consequently the expansion of the previously compressed air became noticeable before the beginning of the pressure increase which accompanied the combustion. Since the engine gave too pointed diagrams at earlier beginnings of the injection, the conclusion must be drawn that it is impossible to obtain ^agood constant-pressure diagram with this cam, and that the cam must therefore be altered.

In the first place, the point of the maximum needle lift must be shifted toward the right, i.e., the crest of the curve must come somewhat later. In this way it is possible to effect a widening of the diagram. This is also apparent from the previ-

ously mentioned diagrams, because the later the crest comes, the wider the diagram is.

In the second place, the needle-lift curve must be somewhat flatter, so that there will not be a too sudden combustion, which is the cause of the pointed indicator diagram.

These are the bases of cam No. 2, Figure 10. Here the needle-lift curve begins at 8° before the dead center, uniformly reaches its maximum lift at 18° after the dead center and ends at 39° after. A series of experiments was also carried out with this cam. The four positions of cam No. 2 are represented by four needle-lift curves (a, b, c, d) in Figure 8, and the needle lift at various crank angles is given in the following table for each position of the cam.

Cam No. 2

Position a		b		c		d	
Crank angle	Needle lift mm	Crank angle	Needle lift mm	Crank angle	Needle lift mm	Crank angle	Needle lift mm
-10°	0	-9°	0	-6°	0	-5°	-
-5°	0.15	-5°	0.07	-	-	-5°	0
Dead center}	0.52	OT	0.35	OT	0.25	OT	0.1
$+5^\circ$	1.12	$+5^\circ$	0.92	$+5^\circ$	0.80	$+5^\circ$	0.64
10°	2.00	10°	1.80	10°	1.62	10°	1.40
15°	2.63	15°	2.4	15°	2.27	15°	2.15
20°	2.64	20°	2.5	20°	2.35	20°	2.20
25°	1.90	25°	2.0	25°	1.80	25°	1.67
30°	0.85	30°	0.97	30°	0.80	30°	0.72
35°	0.10	35°	0.13	35°	0.05	35°	0.05
38°	0	38°	0	36°	0	36°	0

Corresponding to the needle-lift curves (a, b, c and d)

in Figure 8, the indicator diagrams 1, 2, 3 and 4 were made, as shown in Figure 11. The maximum pressure and width of diagram are given in the following table.

Crank angle of injection before dead center	Maximum combustion pressure	Width of indicator diagram
10°	35.5 atg	3.4 mm
9°	35.0	3.6 "
6°	32.8	4.0 "
5°	32.0	5.0 "

Here we already note an improvement in the shape of the diagrams.

1. They are not so pointed as before.
2. The maximum pressure is not so high as before (35.5 against 40 atg), although the injection begins at 10° (instead of 6°, as in the previous case) before the dead center. Here also it is shown that the earlier the injection begins, the more pointed the diagram and the higher the maximum pressure.

Diagram 4 (Fig. 11) has an injection 5° before dead center. If we assume that the hatched portion belongs to the diagram, i.e., that the combustion line would run around it, we would then have a satisfactory diagram. It would then no longer be pointed, but quite wide and, moreover (which is the most important consideration), the maximum pressure would be only 32 atg, i.e., the pressure increase during the combustion would be only 3 atm (32-29).

The question now is, as to how the needle-lift curve must be altered, in order to include the lacking area. It is clear that, in the beginning, more of the mixture of fuel and air must be delivered, i.e., the needle-lift curve must be somewhat higher than the d curve in Figure 8. The point of maximum needle lift must also be somewhat shifted, up to 20° after the dead center.

With this knowledge, a new cam No. 3 was designed, as represented in Figure 12. The same cam is represented in Figure 8 by a dot-and-dash line, in order to show the deviations from the various positions of the preceding cam. Good diagrams (Fig. 13) were obtained with this cam in the same engine, which had previously yielded the pointed diagrams shown in Figure 13a. This great improvement in the shape of the diagram was therefore made simply by altering the shape of the cam, from which the important influence of the correct shape of this engine part on the indicator diagram is clearly recognizable. The needle lifts for cam No. 3, at various crank angles, are as follows.

Cam No. 3

Crank angle in degrees	Needle lift in mm
-10	0.00
- 5	0.50
Dead center }	0.52
+ 5	0.72
10	1.40
15	2.15
20	2.40
25	2.00
30	1.30
35	0.50
40	0.00

Even the diagrams with cam No. 3, in spite of their considerable improvement, are not ideal, because, with their blunt roundings, they are not perfect constant-pressure diagrams. The experiments were therefore continued, until we finally succeeded in obtaining an almost perfect constant-pressure diagram (Fig. 15). The corresponding cam shape is easily deduced from the needle-lift curve in Figure 14. The needle lifts for the new cam No. 4, at various crank angles are as follows.

Cam No. 4

Crank angle in degrees	Needle lift in mm
-15	0.00
-10	0.05
- 5	0.20
Dead center }	0.52
+ 5	1.07
10	1.72
15	2.30
20	2.52 max.
25	2.20
30	1.45
35	0.61
40	0.00

I will designate this cam as the ideal or normal cam. It serves as the basis for calculating the shape of the cam for any engine. As we can see in the design of a cam, the revolution speed of an engine plays a part in the determination of the injection period, while the size of the engine has practically no influence on the computation and the design of a cam. This is due to the fact that the combustion processes have a common basis,

which is determined by the character of the cam and of the atomizing device. The question of the cam shape will be more thoroughly discussed later.

The needle velocity has an important bearing on the development of the cam shape. The needle velocity was determined by the differentiation of the needle-lift curve and is given for all four cams in the following table.

Cam No. 1		Cam No. 2		Cam No. 3		Cam No. 4	
Crank angle	Needle velocity dcm/sec						
-15°	-	-8°	0	-10°	0	-15°	0
-10°	-	-5°	0.05	-5°	0.45	-10°	0.3
-5°	0	-5°	0.05	-5°	0.45	-5°	0.84
Dead center	3.15	0T	1.95	0T	1.5	0T	1.95
+ 5°	4.80	+5°	3.24	+5°	2.85	+5°	2.94
10°	3.75	10°	4.35	10°	3.54	10°	3.00
15°	0	15°	2.7	15°	2.4	15°	2.55
20°	2.70	18°	0	20°	0	20°	0
25°	3.95	25°	3.6	25°	2.7	25°	3.0
30°	4.20	30°	4.8	30°	3.6	30°	4.2
35°	0.75	35°	2.7	35°	3.3	35°	3.9
36°	0	39°	0	40°	0	40°	0

In Figures 6, 10, 12 and 14 the needle velocities for four cams are plotted against the crank angle or time, and the needle-velocity curves are developed therefrom. The velocity curve for cam No. 1 (Fig. 6) climbs very rapidly to its maximum value, 48 cm (1.57 ft.) per second. The velocity curve climbs much slower for cam No. 2 (Fig. 10), and the maximum velocity of 43 cm (1.41 ft.) per second is reached at 10° after the dead

center. For cam No. 4 (Fig. 14) we note a remarkable course of the velocity curve. After a slow climb to 5° past the dead center, the curve (which began at 15° before the dead center, instead of 10, 8, or 5° before, as in the previous cases) reaches its maximum value of about 30 cm (0.98 ft.) per second and remains constant up to 13° after the dead center and then drops to zero at 20° after the dead center. For the descending portion of the needle-lift curve, the character of the velocity curve remains much the same. For reasons to be given later, this portion of the curve received no special attention.

It was found that the ascending branch of the needle-lift curve must show the closest possible agreement with the plotted curve. On the other hand, experience has shown that moderate deviations from the needle-lift curve in the descending portion have no particular effect on the indicator diagram. This is due to the fact that most of the fuel charge is injected during the first part of the needle-lift curve. Figure 15a contains two cam curves which show great similarity in the ascending branch, but considerable deviations in the descending branch. By shifting diagram 2 by a crank angle of one degree, which would scarcely affect its shape, the first part of the cam curve can be made to coincide almost perfectly with the corresponding portion of diagram 1. The indicator diagrams (Fig. 15a) obtained for these cam shapes show only negligible differences in the essential points, which is sufficient proof that no great importance needs

to be ascribed to the descending portion of the curve.

The position of the maximum needle lift, the so-called "crest" of the needle-lift curve, also has an especial influence on the indicator diagram. In order to investigate this rightly, an experiment was tried. A cam was made as shown in Figure 16. This cam began at 12° before the dead center and was arranged so that the position of the crest was adjustable, while the beginning of the injection could be kept constantly at 12° before the dead center. For the position of the crest at 20° after the dead center, diagram 2 (Fig. 17) was obtained and, for 25° after the dead center, diagram 1 (Fig. 17). It is manifest that any position of the crest beyond 20° after the dead center is unfavorable for the shape of the indicator diagram. The position of the crest before 20° after the dead center likewise yields poor diagrams, as was shown by the previous experiments. The conclusion must therefore be drawn that the best location for the maximum needle lift is $18-20^\circ$ after the dead center.

As already mentioned, the fuel injection is generally almost completed when the maximum needle lift is reached. Consequently, the quickest possible closing of the valve through the line a b in the needle-lift curve (Fig. 14) would be theoretically advisable, in order to effect a favorable injection-air consumption. Such a sudden closing of the valve is not feasible, however, due to the tremendous acceleration of the needle it would necessitate. Some time must therefore be allowed, after the maximum lift, for

the gradual descent of the needle-lift curve. It is, however, desirable to close the valve as soon as feasible after the maximum lift, in order to obtain the most favorable injection-air consumption and a corresponding improvement in the mechanical efficiency.

We can designate the following points as the characteristic points of the cam or needle-lift curve:

- 1) Beginning of injection;
- 2) Lift at dead center;
- 3) Point of maximum lift;
- 4) End of injection.

The first three points are especially important and greatly affect the indicator diagram. Hence, from point 1 to point 3, the cam must be accurately made to within 0.01 mm (0.0004 in.). As regards point 4, it can only be said that it should be as near as possible to point 3. For the design and calculation of the cam, we can take the points on the ideal or normal needle-lift curve, which have already been mentioned, namely:

- 1) The needle lift begins at 15° before the dead center;
- 2) The needle lift at the dead center is 0.5 mm (0.02 in.) for a maximum lift of 2.5 mm (.098 in.);
- 3) The crest of the needle-lift curve lies at $18-20^\circ$ after the dead center;
- 4) The valve closes at 40° after the dead center.

After these points and the course of the curve with refer-

ence to the normal curve have been determined, it is very easy to determine the needle-lift curve for various maximum needle lifts, as was done in Figure 18 for 2.5, 3.5 and 4.5 mm (.098, .138, and .177 in.) maximum needle lift. In this manner it is possible to plot at once the needle-lift curve corresponding to any desired maximum needle lift and therefrom to determine the shape of the cam. The needle lift for various crank angles can likewise be derived in % of the maximum lift from the normal curve, and needle-lift curves of any desired maximum needle lift can thus be easily plotted. In the following table, the needle lift is expressed in % of the maximum lift in terms of the crank angle.

Crank angle	% of maximum lift
15° before dead center	0
10° " " "	2
5° " " "	8
At dead center	21
5° after dead center	42
10° " " "	68
15° " " "	92
20° " " "	100
25° " " "	88
30° " " "	58
35° " " "	26
40° " " "	0

For example, at the dead center the needle lift is

$$ht = 0.21 \times 4 = 0.84 \text{ mm (0.033 in.)}$$

with a cam which would give a maximum lift of 4 mm (0.157 in.).

Furthermore, by planimetry from the normal curve I found the mean lift to be 1.18 mm (0.046 in.). In this case the maximum needle lift is 2.5 mm (0.098 in.). Hence

$$\rho = \frac{\text{max. needle lift}}{\text{mean needle lift}} = \frac{2.5}{1.18} = 2.12.$$

After this ratio has been established once for all, the maximum needle lift can be easily determined from the mean needle lift, and the needle-lift curve from the maximum needle lift, as has already been mentioned, which determines the shape of the cam. This fact is very important for the designer. I will take up the determination of the mean needle lift later.

As regards the valve seat, we find that the narrowest cross section is located at x in Figure 21. This is likewise the narrowest cross section in the whole valve. The same is also apparent on Figures 3 and 5. This cross section, however, is variable. It increases from zero, when the valve is closed, to its maximum value at the maximum needle lift and then drops again to zero at the end of the needle-lift curve. The question is now to determine the curves from which the cross sections can be read for various needle lifts and vice versa. It is obvious that this cross section depends on the needle lift h , the angle of slope α and the diameter d of the discharge passage. The angle α

is assumed to be 45° for all engines, as otherwise there would be a series of curves for each value of α . Mathematically expressed, we therefore have the cross section $q = (d - 2r)\pi \beta$ according to Figure 21, where β (the perpendicular distance of the valve-seat surface from a) = $h \sin \frac{45}{2} = 0.3827 h$ (h = needle lift). r = projection of $\beta/2$ on $a - b = \frac{\beta}{2} \cos \frac{45}{2} = 0.924 \frac{0.3827}{2} h$. Hence $2r = 0.924 \times 0.3827 h = 0.354 h$.

If I keep the discharge passage diameter $d = 6$ mm (0.236 in.) constant, and calculate the cross section q for different values of the needle lift from zero to 4 mm (0.157 in.) (which it should not exceed), I obtain the cross section at various needle lifts corresponding to the discharge-passage diameter of 6 mm (0.236 in.). This result I plotted in Figure 19. In like manner the cross sections for discharge-passage diameters of 10 and 16 mm (0.394 and .63 in.) can be determined and the corresponding curves plotted, as was done on the same figure. The following table contains the numerical values of these cross sections.

Needle lift in mm	β	2r	6-2r	q in mm ² for d=6	10-2r	q in mm ² for d=10	16-2r	q in mm ² for d=16
0	0	0	6	0	10	0	16	0
0.5	0.1913	0.177	5.829	3.5	9.823	5.9	15.823	9.5
1.0	0.383	0.354	5.646	6.74	9.646	11.5	15.646	18.8
1.5	0.574	0.53	5.47	9.85	9.47	17.0	15.47	27.8
2.0	0.765	0.707	5.293	12.7	9.293	22.3	15.29	36.7
2.5	0.956	0.835	5.115	15.38	9.115	27.4	15.12	45.4
3.0	1.15	1.06	4.94	17.84	8.94	32.4	14.94	54.0
3.5	1.34	1.24	4.76	20.1	8.76	36.8	14.76	62.1
4.0	1.53	1.415	4.585	22.0	8.585	41.2	14.59	70.0

I designate the curves in Fig. 19 as cross-section curves. They are indispensable for designing the cam. With the aid of these curves, it is very easy to determine the needle lift for a given cross section, for the discharge-passage diameter under consideration, and vice versa. It is advisable to plot a number of such curves for the different discharge-passage diameters which may come under consideration.

As the basis for the conception of the mixing ratio, which can be variously established, I give the following definition.

It is the ratio of the volume of the injection air at 60 atm. and 20°C (68°F) to the volume of the fuel which flows through the valve in one and the same atomization process during a single injection. I have included this volume in the calculation, because it facilitates the consideration of the phenomena. I calculated this ratio v from the fuel and injection-air consumption of several engines of different sizes and revolution speeds and found that the ratio depends only on the revolution speed and

has the following values:

$$v = 25.0 \text{ at } n = 400 \text{ R.P.M.}$$

$$v = 21.5 \text{ " } n = 300 \text{ "}$$

$$v = 15.0 \text{ " } n = 125 \text{ "}$$

I plotted these ratios against the R.P.M. as shown in Figure 20. The result is an almost straight line, showing that the mixing ratio (i.e., the specific injection-air consumption) increases directly as the R.P.M. of the engine. This agrees with our expectations because, with increasing R.P.M., the available time for atomization and combustion constantly decreases. At 400 R.P.M. the injection period is only 0.023 sec. and at 125 R.P.M. it is 0.0734 sec. The requisite equalization can here be obtained by increasing the specific injection quantity.

The fuel consumption for the indicated horsepower-hour corresponds to the indicated thermal efficiency of the engine which, with like specific load (like mean indicated pressure) within the speed limits of Diesel engines, is only slightly dependent on the R.P.M., but somewhat more on the size of the engines (cooling; ratio of volume to surface area of combustion chamber). In these investigations a mean value of 145 g (0.32 lb.) per $HP_i/\text{hr.}$ was found for the different types, whereby the deviations were less than 5%. This value corresponds to an indicated thermal efficiency of about 45%. Values agreeing with this often occur in the literature on this subject. Deviations from this order of magnitude are of no special significance for

the determination of the height of the cam, so that calculations can be made unhesitatingly with the above mean value.

From the above principles, I would like to make the calculation for the design of a fuel-valve cam.

Example 1. - It is desired to design a fuel cam for a one-cylinder four-stroke-cycle engine of 460 HP_i with $n = 125 \text{ R.P.M.}$, $D = 740 \text{ mm (29.13 in.)}$, $H = 1200 \text{ mm (47.24 in.)}$, with disk atomizer.

The mean fuel consumption is assumed to be 145 g (0.32 lb.) per $\text{HP}_i/\text{hr.}$ Then the fuel injected per working cycle is

$$\frac{460 \times 145 \times 2}{60 \times 125} = 17.7 \text{ g (0.039 lb.)} =$$

$$= 20.6 \text{ cm}^3 \text{ (1.26 cu.in.) at } \gamma = 0.86 \text{ g/cm}^3 \\ \text{for gas oil}$$

From the curve in Figure 20, the mixing ratio is found to be 15. Hence the injection-air volume per cycle is $20.6 \times 15 = 310 \text{ cm}^3$ (18.92 cu.in.) at 60 atm. and 20°C (68°F).

This volume of air flows through the narrowest cross section of the valve seat at x (Fig. 1) and expands up to a counter-pressure of 30-35 atm. This is assumed to remain constant at 35 atg, although it varies somewhat during the injection process. The variation in the temperature of the air during this process is difficult to follow. On the one hand, the air receives heat from the walls while, on the other hand, the temperature falls, because of the expansion to the final compression pressure. If we assume that the intake and outgo of heat offset each other,

i.e., that the temperature of the injection air remains constant at 20°C during its flow through the narrowest cross section, the volume of the outflowing air is found to be

$$310 \times \frac{61}{36} = 525 \text{ cm}^3 \text{ (32.04 cu.in.)}.$$

The fuel volume = 20.6 cm³, as already determined. Hence the volume of the mixture is

$$V = 525 + 20.6 = 545.6 \text{ cm}^3 \text{ (33.29 cu.in.)}.$$

The narrowest cross section must let this volume pass through during the injection period.

From the flow formula for air (in the subcritical region $p_0/p_1 > 0.53$) we obtain the velocity

$$w_0 = \varphi \sqrt{2g \frac{k}{k-1} p_1 v_1 \left[1 - \left(\frac{p_0}{p_1} \right)^{\frac{k-1}{k}} \right]}$$

(φ = velocity coefficient)

with $p_1 v_1 = R T_1$, in which p_1 , v_1 , T_1 represent the original condition of the air and p_0 the final pressure

$$k = 1.4; R = 29.27$$

$$w_0 = 44.8 \varphi \sqrt{T_1 \left[1 - \left(\frac{p_0}{p_1} \right)^{0.286} \right]}$$

in which $T_1 = 20 + 273 = 293^\circ$ abs.

$p_0 = 35$ atg. = 36 atm. abs.

$p_1 = 60$ " = 61 " "

With the values assumed for T and for p_0/p_1 , it was necessary to put $\varphi = 0.8$, in order to obtain an agreement of the air quantities (calculated with the help of the above out-

flow formula) with the measured volumes. Hence $w_0 = 232$ m (761 ft.)/sec.

As we know, the needle lift begins at 15° before the dead center and ends at 40° after, thus covering a crank angle of 55° . The injection period is therefore $\frac{55 \times 60}{125 \times 360} = 0.0734$ sec.

The air, which must flow with a velocity of 232 m/sec in 0.0734 sec. ($V = 545.6$ cm³), requires a cross section of

$$q = \frac{545.6}{232 \times 0.0734} = 32.0 \text{ mm}^2.$$

We have already seen that this cross section depends on the needle lift. In each working cycle it increases from zero to a maximum and then returns to zero. Consequently, the calculated cross section must be regarded as the mean cross section.

If we now consider the cross-section curves (Fig. 19), we find that the cross section of 32 mm², (.05 sq.in.) for a discharge-passage diameter of 10 mm (.394 in.) requires a mean needle lift of 2.99 mm (.118 in.), which indicates a maximum needle lift of $2.99 \times \rho = 2.99 \times 2.12 = 6.34$ mm (.25 in.). This is too high. Consequently, I take the channel diameter of 16 mm and the corresponding mean needle lift of 1.73 mm (.068 in.) from the cross-section curve. Thus I obtain the maximum needle lift of $2.12 \times 1.73 = 3.67$ mm (.144 in.). We can now plot the needle-lift or cam curve on the basis of the ideal or normal curves, as already explained.

Crank angle	Needle lift in mm
15° before dead center	3.67 x 0 = 0
10° " " "	3.67 x 0.02 = 0.073
5° " " "	3.67 x 0.08 = 0.29
At dead center	3.67 x 0.21 = 0.77
5° after dead center	3.67 x 0.42 = 1.54
10° " " "	3.67 x 0.68 = 2.49
15° " " "	3.67 x 0.93 = 3.38
20° " " "	3.67 x 1.00 = 3.67
25° " " "	3.67 x 0.88 = 3.22
30° " " "	3.67 x 0.53 = 2.12
35° " " "	3.67 x 0.26 = 0.954
40° " " "	3.67 x 0 = 0

This gives the needle-lift curve, from which the cam shape can be developed as the enveloping curve of the tappet roller. It should, however, be borne in mind that this curve is based on a roller play of zero. In order to allow for the roller play, the curve must be prolonged at both ends by tangents to the base circle. In the development, the base circle appears as a parallel to the zero line at the distance of the roller play, which can have a value up to 1 mm according to the size of the engine (Fig. 22).

In this connection, it should also be mentioned that the peripheral velocity of the cam disk lies between 1.5 and 2 m per second and that the ratio of the disk diameter to the roller diameter is assumed to be 4 - 5. With a peripheral velocity of 1.5 m/sec

$$d = \frac{1.5 \times 1000 \times 60 \times 2}{\pi \times 125} = 460 \text{ mm}$$

and the roller diameter = $\frac{460}{5}$ = about 90 mm (3.54 in.).

Calculation of the important dimensions.— The diameter of the discharge passage has already been established in designing the cam. In order to determine the height of the discharge passage, 1.25 was adopted as the ratio of the height of the passage to its diameter. This ratio applies to all engines and has yielded good results in practice. The height is determined by the conditions that, on the one hand, the needle must not come too close to the nozzle and, on the other hand, that the total height of the valve must be kept as small as possible. As the height of the passage, we thus obtain $1.25 \times 16 = 20$ mm (.787 in.) (Fig. 4).

The needle is given about twice the diameter of the discharge passage. Thus $d_N =$ about $2 \times 16 = 32$ mm (1.26 in.) (31 mm (1.22 in.) being adopted in Fig. 4).

The diameter D of the valve cage (Fig. 4) is about 2.25 times the diameter of the needle and depends, moreover, on the diameter of the atomizer disks, on the necessary cross section through the disks and on the thickness of the casing. $D = 2.25 \times 31 =$ about 70 mm (2.76 in.) (Fig. 4).

Valve-spring tension.— By differentiating the needle-lift curve (Fig. 22), we obtain the needle-velocity curve and therefrom, by a second differentiation, the needle-acceleration curve. We thus obtain a maximum needle acceleration of 67.6 m (221.8 ft.)/sec. The combined weight of the needle and disks is about 11.5 kg. We thus obtain a valve-spring tension of $\frac{11.5}{g} \times 67.6 =$ 79.5 kg (175.3 lb.). Experience shows that this is much too

small. Consequently I attempted to determine the valve-spring tension empirically. The spring must actually withstand two tensions.

1. The spring must be strong enough to withstand the combustion pressure. This pressure is $\frac{\pi}{4} d^2 \times 35$, if d = needle diameter in millimeters and 35 = combustion pressure in kg/cm^2 .

2. The spring must withstand the acceleration forces of the valve needle and disks. I have introduced this factor as a function of the injection period.

It is advisable to compute the valve-spring tension with the following empirical formula, which contains an adequate safety factor.

$$P = \frac{\pi d^2}{4} \times 35 \times 1.6 \sqrt[4]{\frac{l}{t}}$$

in which t denotes the injection period in seconds. I have compared the valve springs of engines with this formula and found that the deviations were never more than 3%. It should be remembered that the spring tension is adjustable in every engine. Consequently, this formula can be safely used for calculating the valve spring.

$$P = \frac{\pi d^2}{4} \times 35 \times 1.6 \sqrt[4]{\frac{l}{t}} \dots \dots$$

$$P = \frac{\pi 3.1^2}{4} \times 35 \times 1.6 \sqrt[4]{\frac{1}{0.0734}} \cdot$$

As a matter of fact, the spring had a tension of 790 kg (1741.6 lb.)

Nozzle cross section.— For the sake of a regulated flow, the narrowest cross section of the valve should be kept at the point x in Figure 21, even at the maximum needle lift. If the nozzle cross section is kept as small as possible, it can equal the narrowest cross section at the maximum lift. In reality the ratio of the nozzle cross section to the maximum needle-lift cross section is generally somewhat less favorable, namely, 0.9 - 1, without causing any trouble. I here take the mean value, 0.95. The cross section at the maximum needle lift of 3.67 mm (.144 in.) (Fig. 19) is 64.8 mm². Therefore the nozzle cross section = $0.95 \times 64.8 = 61.5 \text{ mm}^2$ (.095 sq.in.). When divided between five nozzle holes, this gives $d = 3.95 \text{ mm}$ (.156 in.) as the diameter of each hole. The nozzle was made with $d = 4 \text{ mm}$ (.157 in.). This makes the ratio of the nozzle cross section to the smallest valve cross section 0.97 at maximum needle lift.

The previously mentioned attempt to investigate the effect of the cam on the indicator diagram and on the combustion was made with a two-cylinder four-stroke-cycle engine of 75 HP_i per cylinder and $n = 400$ R.P.M. with a sleeve atomizer and the results were used for the following four-stroke-cycle engine types:

1. 8-cylinder engine, 460 HP_i per cylinder,

$D = 740 \text{ mm}$ (29.13 in.), $H = 1200 \text{ mm}$ (47.24 in.), $n = 125$ R.P.M.

2. 6 cylinder engine, 258 HP_i per cylinder,

$D = 630 \text{ mm}$ (24.8 in.), $H = 960 \text{ mm}$ (37.8 in.), $n = 115$ R.P.M.

3. 2-cylinder engine, 85 HP_i per cylinder,

$D = 350 \text{ mm}$ (13.78 in.), $H = 360 \text{ mm}$ (14.17 in.), $n = 300$ R.P.M.

4. 3 cylinder engine, 75 HP_i per cylinder,
 $D = 310 \text{ mm}(12.2 \text{ in.})$, $H = 350 \text{ mm}(13.78 \text{ in.})$, $n = 300-400 \text{ R.P.M.}$
 at various loads.

Each engine yielded a faultless diagram, without special trouble in adjusting. From this fact it may be concluded that the established cam characteristic for engines of various sizes and revolution speeds is perfectly practical, at least for four-stroke engines. In order to make this still clearer, I computed, as the first example, an 8-cylinder engine with $460 \text{ HP}_i/\text{cylinder}$, $n = 125 \text{ R.P.M.}$ with disk atomizer, which was actually made with this cam. In conclusion, I will also give the calculation for a 2-cylinder engine of $75 \text{ HP}_i/\text{cylinder}$, $n = 400 \text{ R.P.M.}$ with sleeve atomizer.

Example 2.— A cam is to be designed for a four-stroke-cycle engine with sleeve atomizer, $n = 400 \text{ R.P.M.}$, the specific fuel consumption being 145 g/HP/hr. , as previously assumed. Hence the fuel consumed per working cycle is $\frac{145 \times 75 \times 2}{60 \times 400} = 0.907 \text{ g} = 1.054 \text{ cm}^3 (.0643 \text{ cu.in.})$ at a specific gravity of $\gamma = 0.86$. The mixing ratio, taken from Figure 20 at 400 R.P.M. is $v = 25$. Hence the injection-air volume $= 1.054 \times 25 = 26.4 \text{ cm}^3 (1.61 \text{ cu.in.})$ at 60 atm. and 20°C .

With isothermal expansion, as previously assumed, up to 35 atg counterpressure, the volume of the outflowing air $= 26.4 \times \frac{61}{36} = 44.7 \text{ cm}^3 (2.73 \text{ cu.in.})$.

The cam characteristic is the same as before, i.e., the needle-lift curve begins at 15° before the dead center and ends

at 40° after the dead center. Consequently the injection period
 $= \frac{55 \times 60}{400 \times 360} = 0.023$ sec.

From the previously mentioned formula, the air velocity

$$w_0 = 44.8 \varphi \sqrt{T_1 \left[1 - \left(\frac{p_0}{p_1} \right)^{0.286} \right]} \\ = 232 \text{ m/s } (\varphi \sim 0.8).$$

Therefrom we obtain the mean cross section at the narrowest point x (Fig. 21).

$$q = \frac{44.7 + 1.054}{232 \times 0.023} = 8.56 \text{ mm}^2.$$

This cross section gives a needle lift of 1.3 mm (.051 in.) for a discharge passage diameter of 6 mm (.236 in.). Hence the maximum needle lift is $2.12 \times 1.3 = 2.76$ mm (.109 in.).

From this we can determine the needle-lift curve and establish the cam shape for a roller play of 0.5 - 1 mm, as already explained in the first example (Fig. 22).

With 2 m/s peripheral velocity of the cam disk, we obtain the disk diameter

$$d = \frac{2 \times 1000 \times 60 \times 2}{\pi \times 400} = 191;$$

the disk being made with an actual diameter of 200 mm (7.87 in.). Roller diameter $= 200/4 = 50$ mm (1.97 in.). Height of discharge passage $= 6 \times 1.25 = 7.5$ mm (.295 in.) (Fig. 2). Needle diameter $= 6 \times 2 = 12$, the actual diameter being 12.8 mm (.504 in.). Diameter of valve cage $= 12.8 \times 2.25 = 28.8$, actually 28 mm (1.1 in.).

Tension of spring

$$P = \frac{\pi d^2}{4} \times 35 \times 1.6 \sqrt[4]{\frac{1}{t}} \quad \left\{ \begin{array}{l} d = 1.28 \text{ cm} \\ t = 0.023 \text{ sec} \end{array} \right.$$

from which we obtain $P = 184 \text{ kg}$ (405.7 lb.), the spring being actually made with an initial tension of 176 kg (388 lb.)

For a maximum needle lift of 2.76 mm, corresponding to a discharge passage diameter of 6 mm, the cross section was 16.7 mm^2 (.026 sq.in.). Hence the nozzle cross section $= 0.95 \times 16.7 = 15.8 \text{ mm}^2$ (.024 sq.in.). There were eight holes, from which we calculate the diameter $d = 1.58$, actually made with $d = 1.55 \text{ mm}$ (.061 in.), for which the ratio of the nozzle cross section to the smallest valve cross section at maximum needle lift $= 0.91 \text{ mm}$ (.036 in.).

I have already determined the very important dimensions, diameter, and height of discharge passage, nozzle cross section, needle diameter, valve-cage diameter, spring tension and cam shape, and we have seen how they agree with the corresponding dimensions of actual engines of various revolution speeds, dimensions, and atomizer types.

In conclusion, I attempted to determine the velocities at the points A, a, a_1 , etc. (Figs. 2 and 4). The velocities in the following table can serve as the basis for calculating the atomizer of a new engine. I have assumed that the mixture of fuel and air flows through the cross sections under constant conditions of temperature and pressure. Of course some changes occur, but they cannot be numerically evaluated. With this assumption

tion I have established the velocities of the mixture at the different points as follows.

Point	Atomizer type	Velocity in m/sec
A	Disk	3.22
	Sleeve	6.9
a	Disk	2.3
	Sleeve	27.8
a ₁	Disk	2.3
	Sleeve	3.96
b	Disk	13.3
	Sleeve	11.4
c	Disk	2.3
	Sleeve	17.0
d	Disk	20.0
	Sleeve	27.1
e	Disk	20.0
	Sleeve	31.2

In the injection-air pipe (not shown in the diagram), the air has a velocity of 13.4 m (43.96 ft.)/sec. with a disk atomizer and 12.1 m (39.7 ft.)/sec. with a sleeve atomizer. These velocities in the air pipe are naturally independent of the atomizer type. The calculations are made with 10-15 m (32.8-49.2 ft.)/sec.

Approximate velocities for computing the valve cross sections.

Points according to Figs. 3 and 4	Velocities in m/sec	
	Sleeve atomizer	Disk atomizer
A	6-8	3-4
a	2-3	25-30
a ₁	3-4	2-3
b	10-15	10-15
c	15-20	2-3
d	25-30	20-25
e	25-30	20-25

Some deviation is admissible in the fuel-valve cross sections, but a deviation of even 0.1 mm in the needle lift may make trouble.

Conclusion.— The characteristic constant-pressure diagram for the Diesel engine is always the desirable ideal diagram. The pointed diagrams, often obtained, have the disadvantage that the combustion pressure climbs very high and the engine must be made correspondingly heavy. The most recent method of pure mechanical injection is worse in this respect, because the maximum pressure must be raised to over 50 atm. (835 lb./in.²), in order to obtain a favorable specific fuel consumption. Engines which give pointed diagrams often knock and run hard.

With a normal load the specific fuel consumption of an engine with a pointed diagram is not always poor but, as soon as more fuel is introduced, the engine often begins to smoke. This indicates that the overloading of the engine is accompanied by poor combustion. On the contrary, an engine with a constant-pressure diagram runs more smoothly, can be overloaded, and does not smoke at full load nor even with overload.

Moreover, for an engine with pointed diagrams, the compression pressure can hardly exceed 29 atm., while constant-pressure engines can attain a compression pressure up to 33 atm. because the pressure increase during the combustion is not very high (3-4 atm.), thus making possible an improvement in the thermal efficiency.

It is generally known that a compressorless engine suffers under a pointed diagram. Possibly an approximate constant-pressure diagram combined with good combustion can be attained even in compressorless engines.

Translation by Dwight M. Miner,
National Advisory Committee
for Aeronautics.

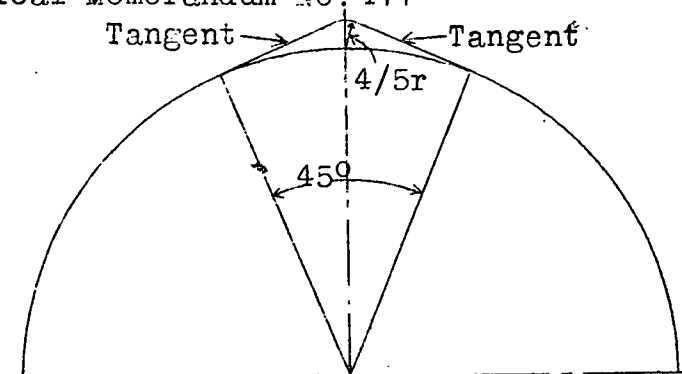


Fig. 1

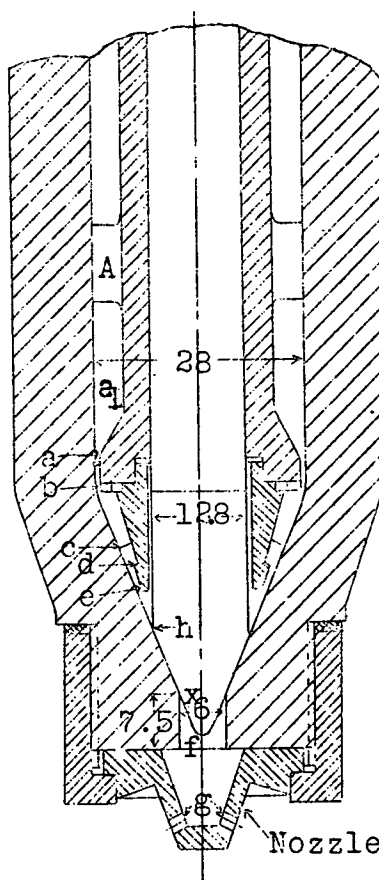


Fig. 2 Sleeve atomizer.

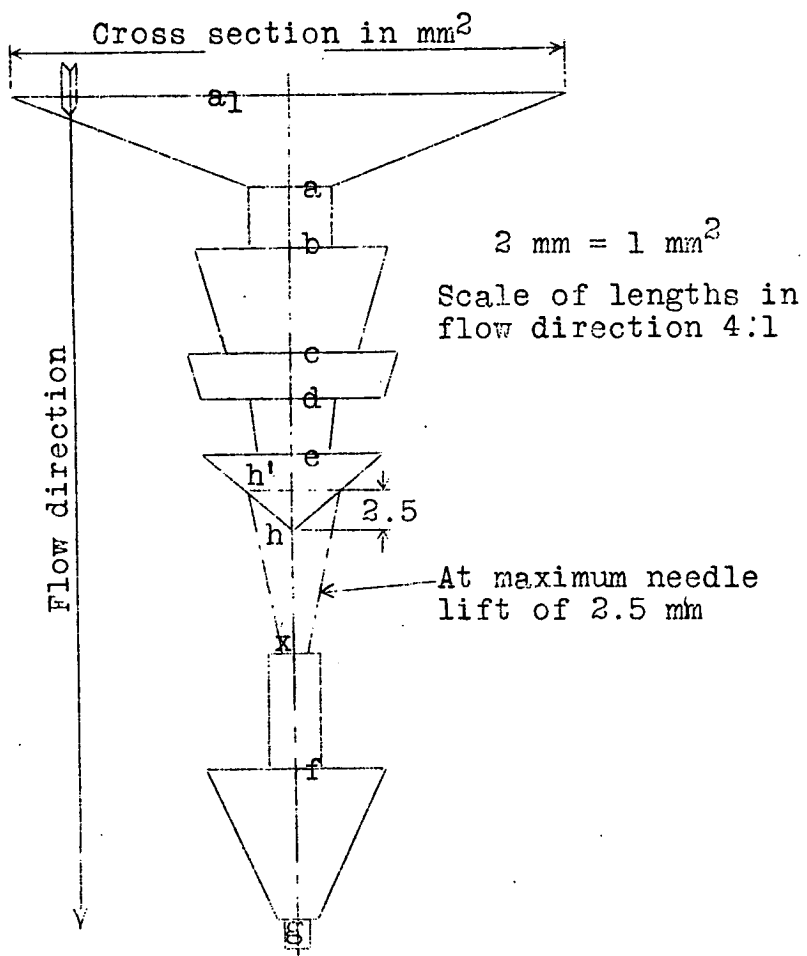


Fig.3 Cross section course of sleeve atomizer.

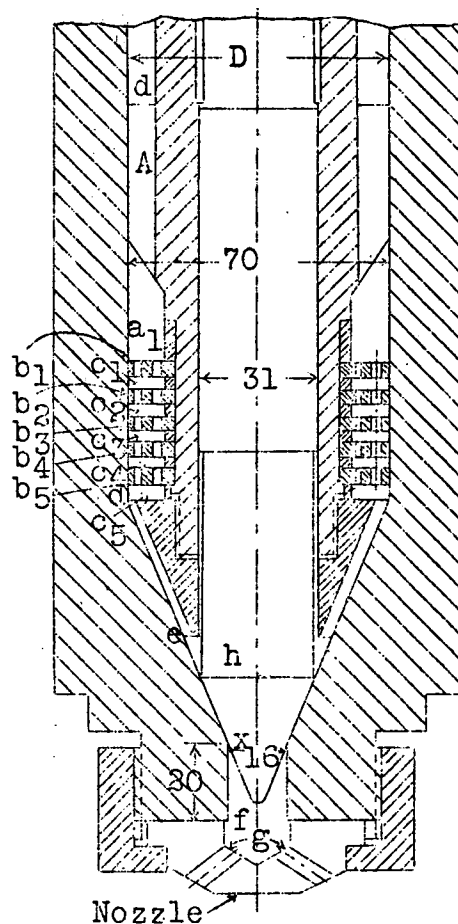


Fig.4 Disk atomizer.

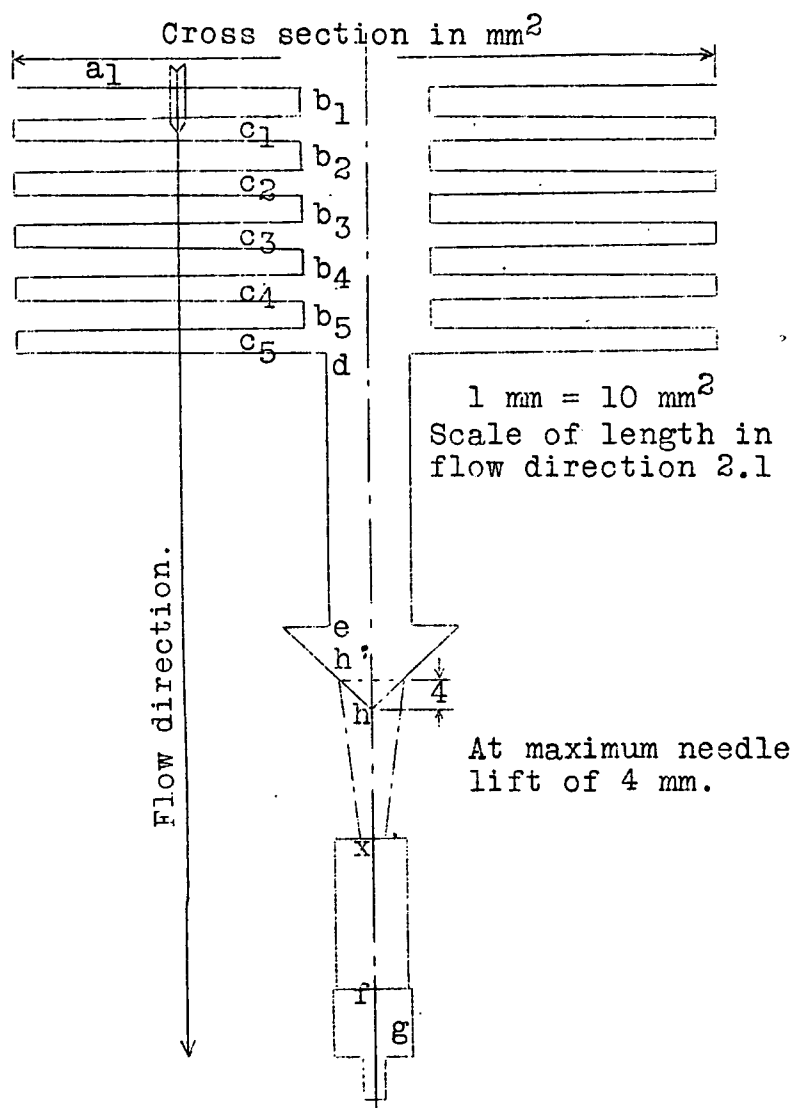


Fig.5 Cross-section course of disk atomizer.

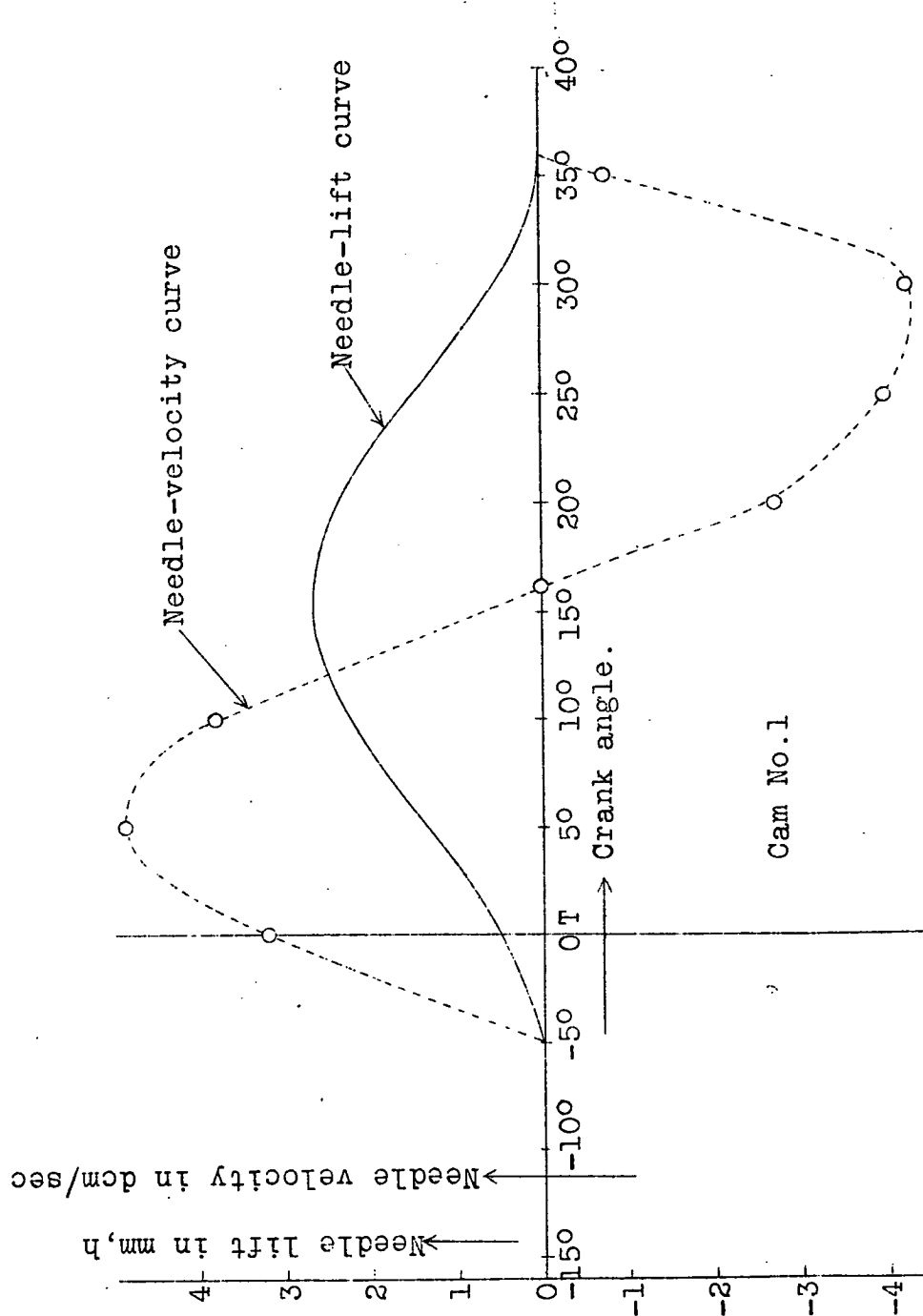


Fig. 6

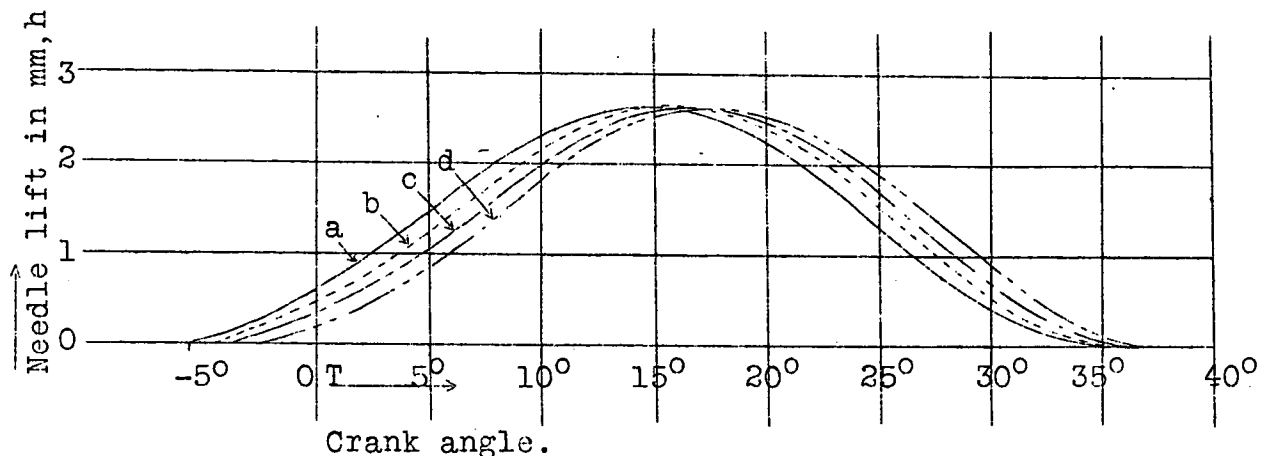


Fig.7

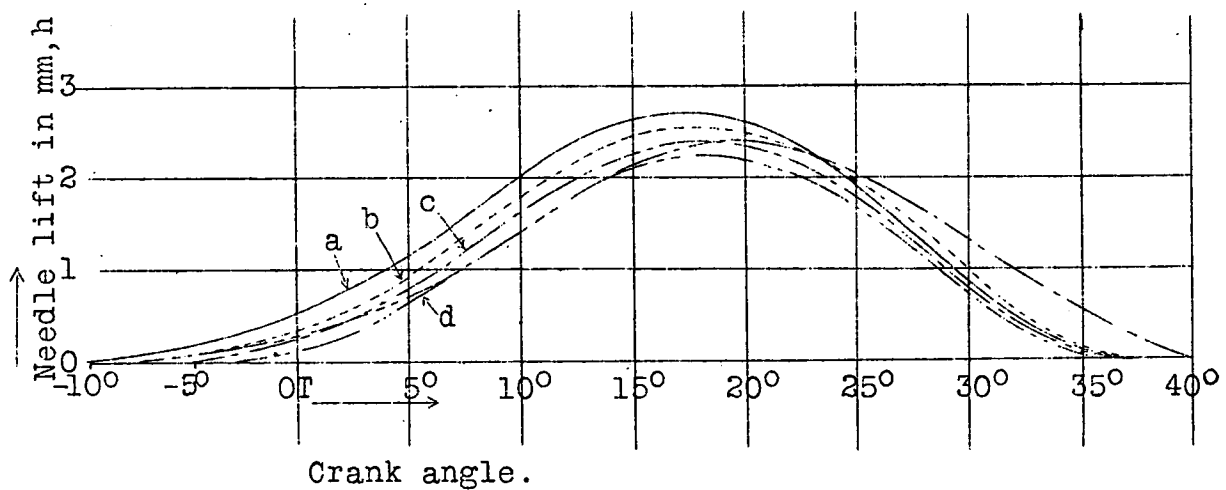


Fig.8

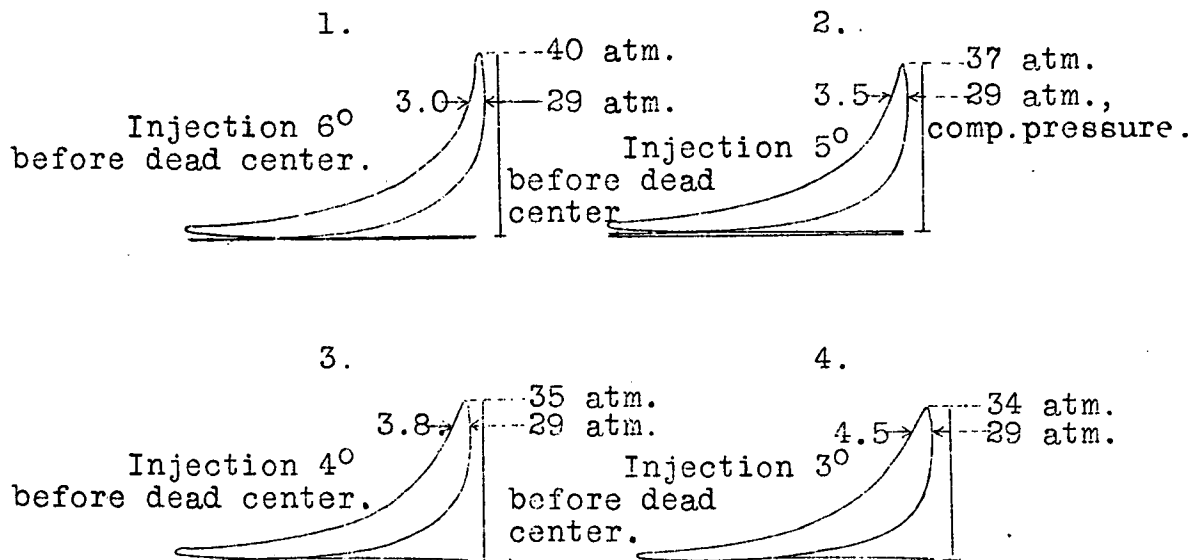


Fig.9

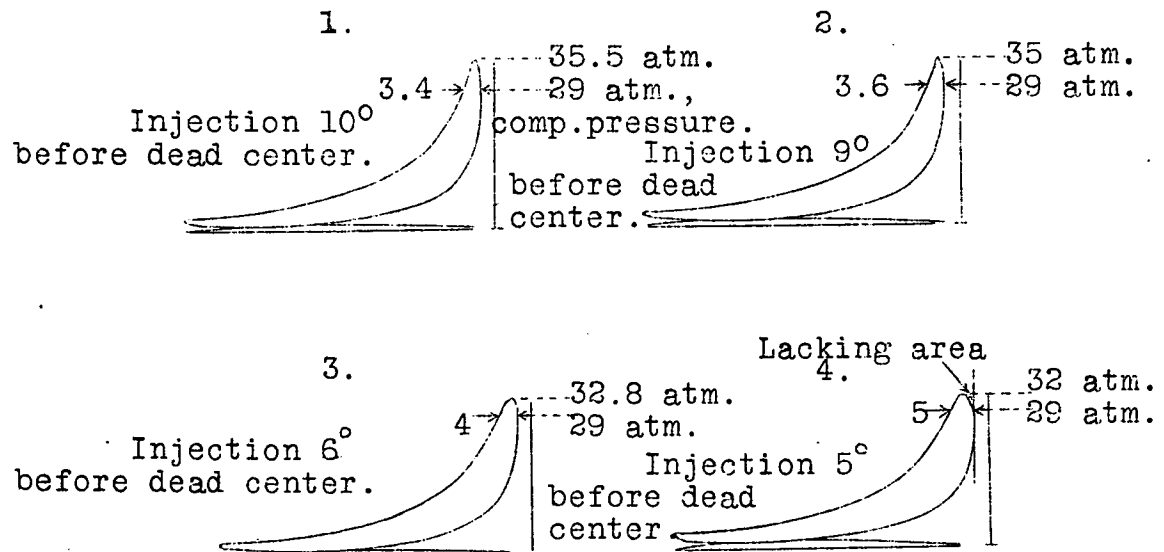


Fig.11

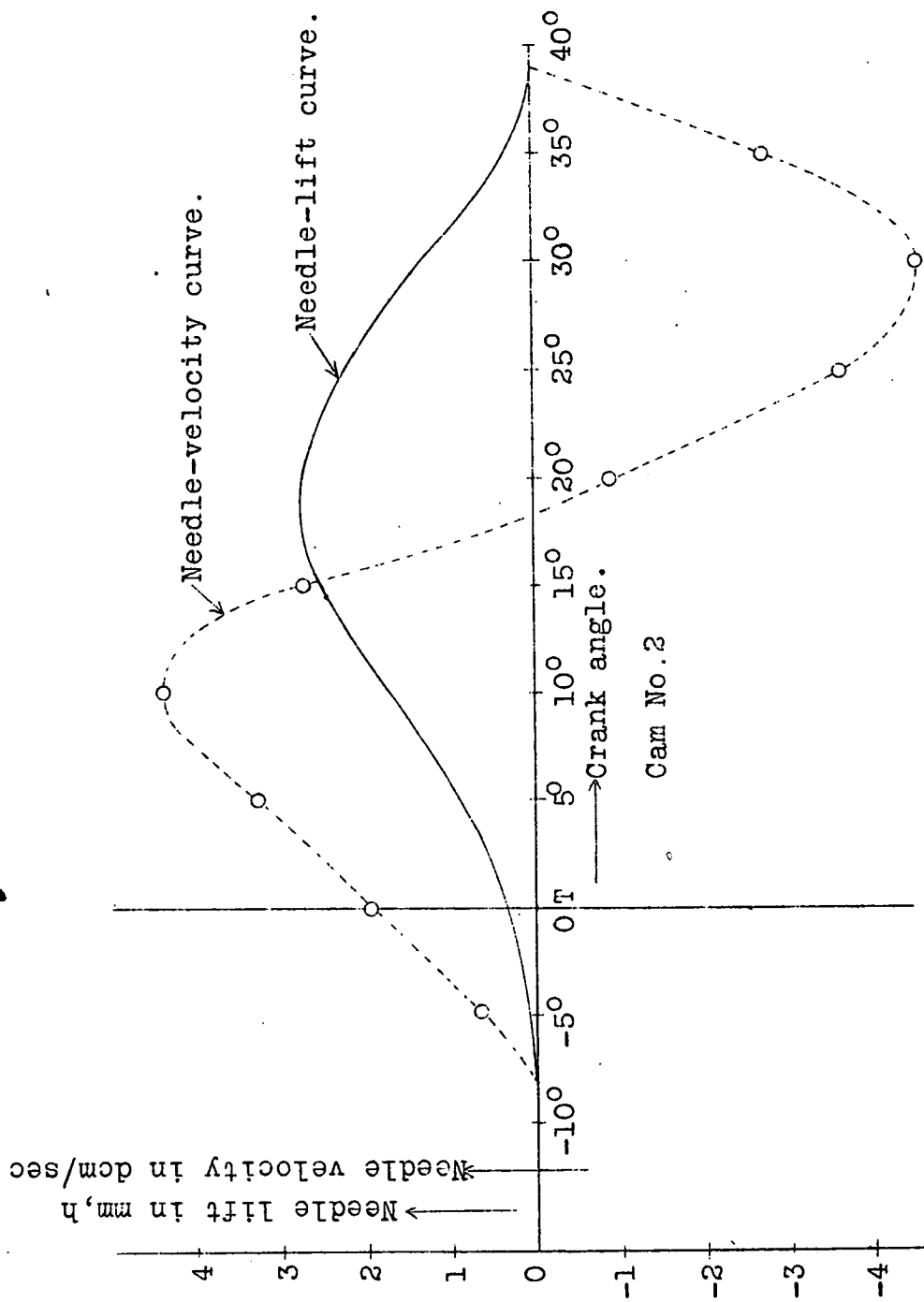


Fig. 10

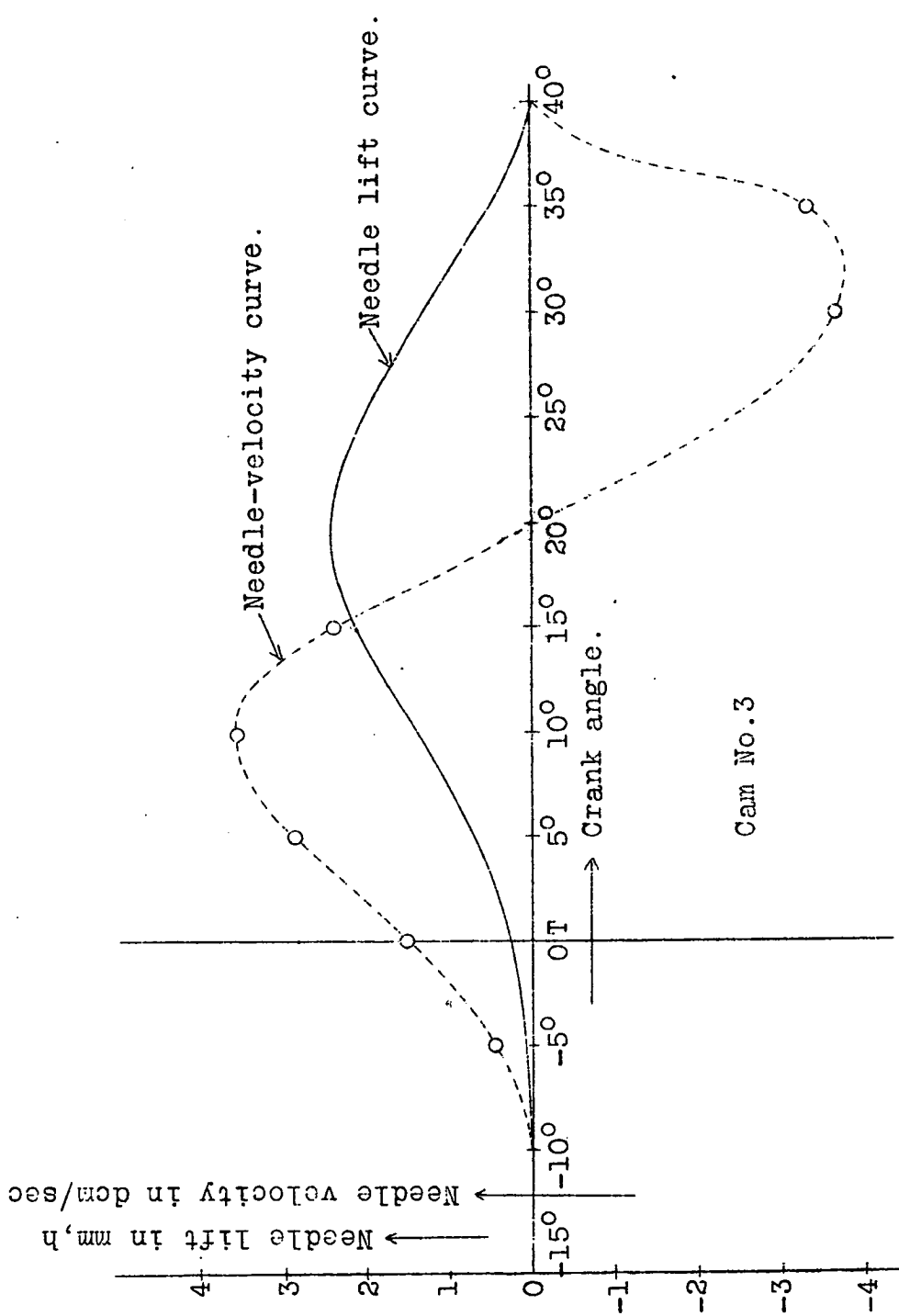


Fig.12

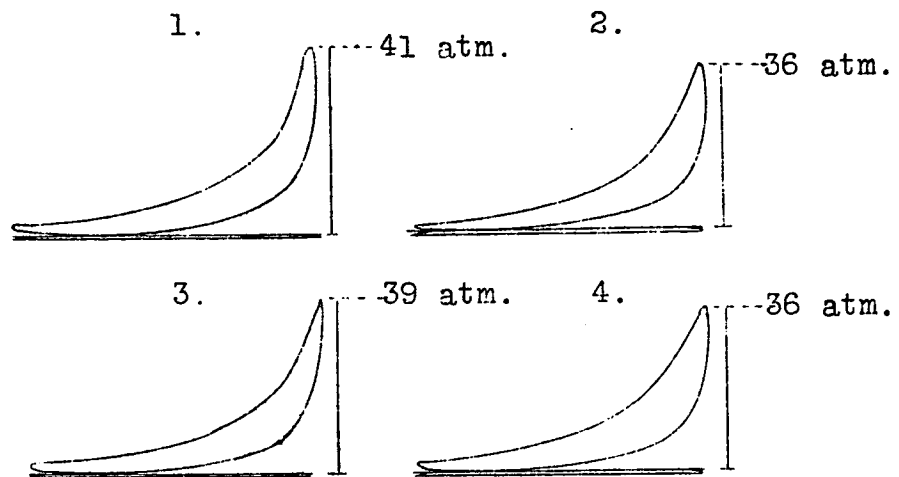


Fig.13a

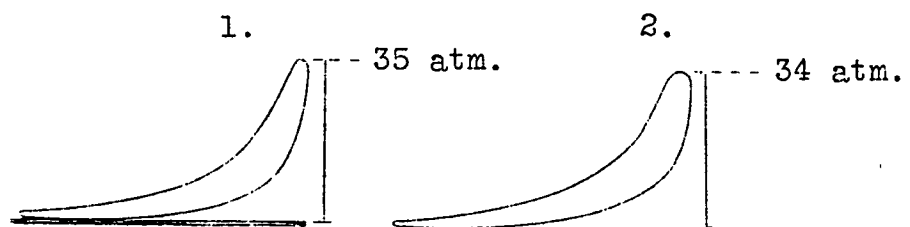


Fig.13

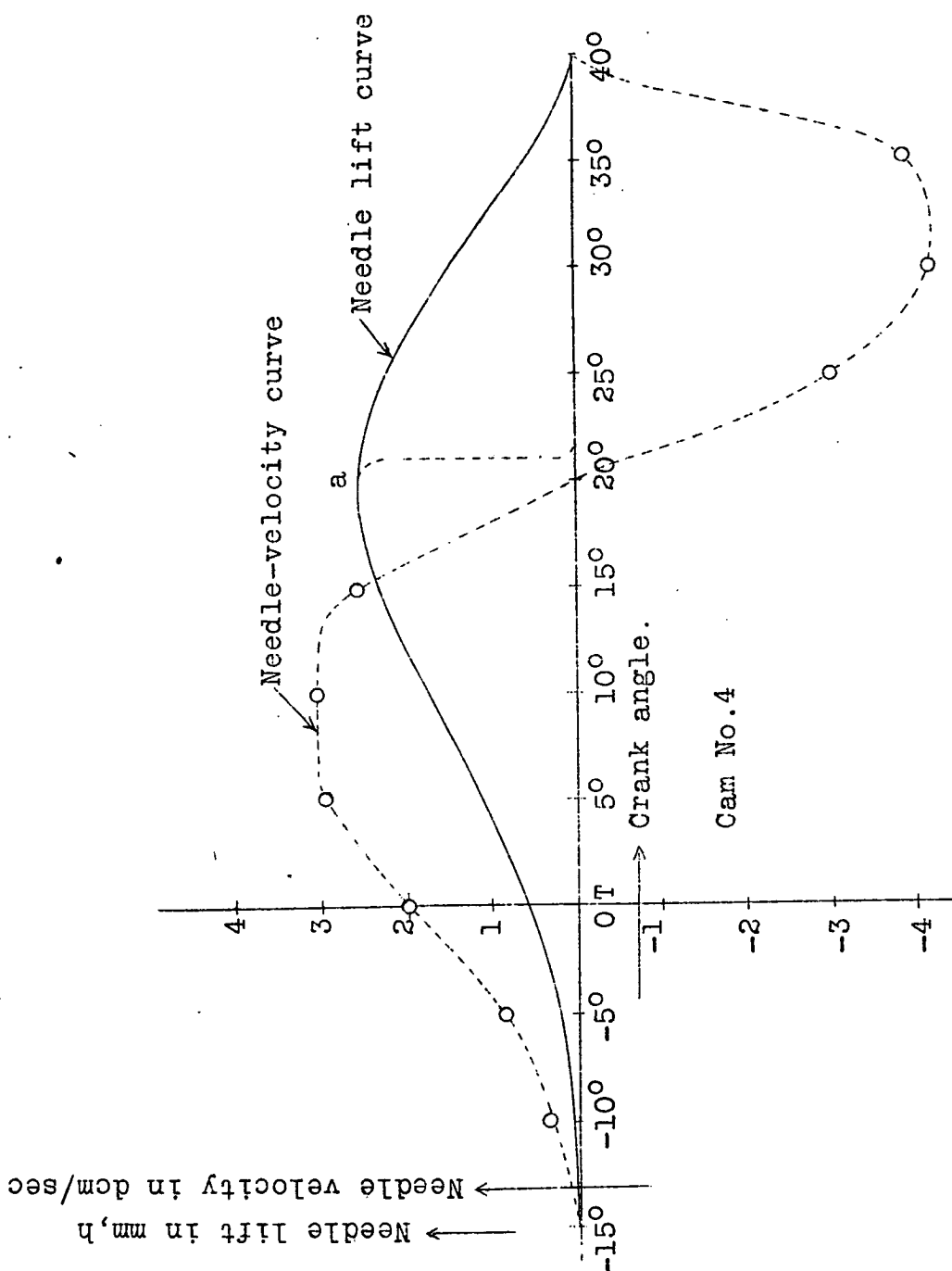


Fig.14

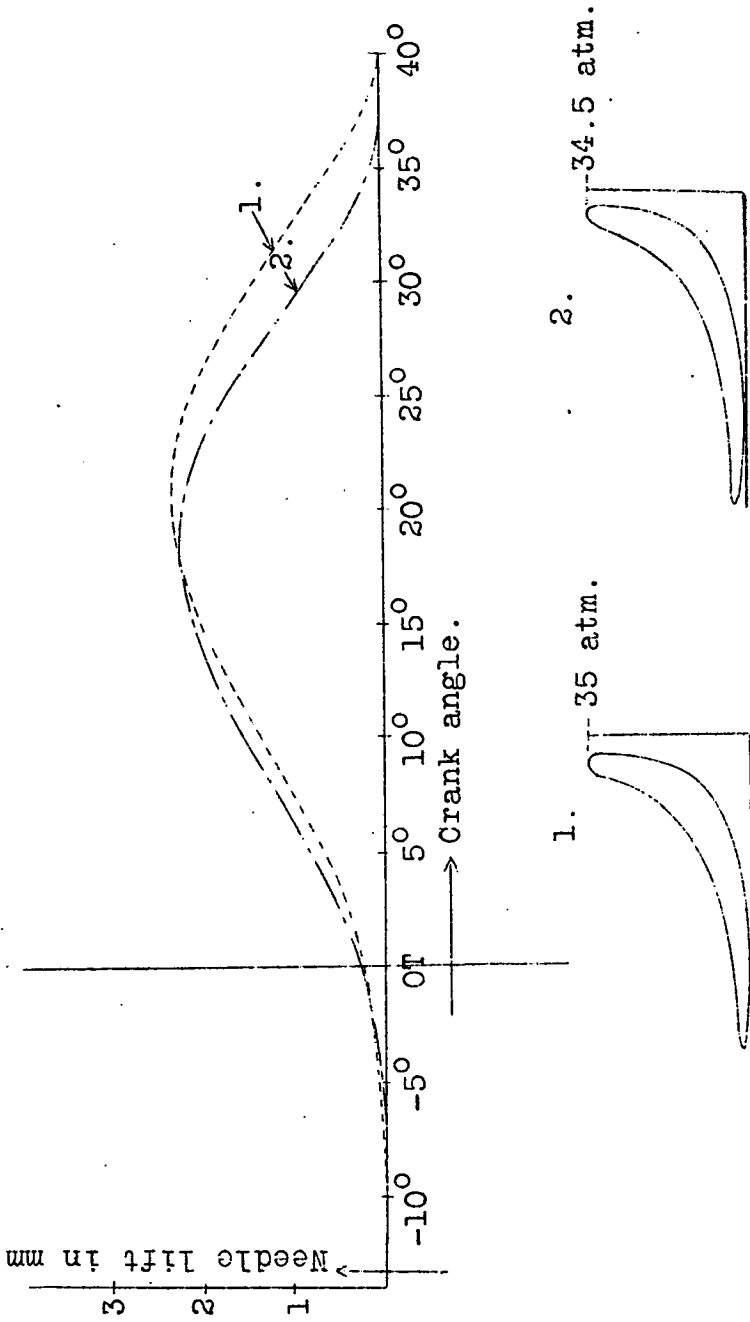


Fig. 15a

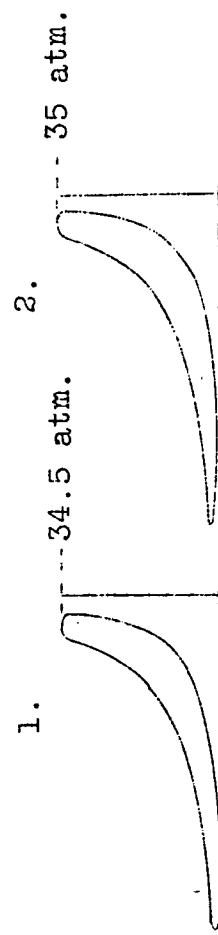


Fig. 15

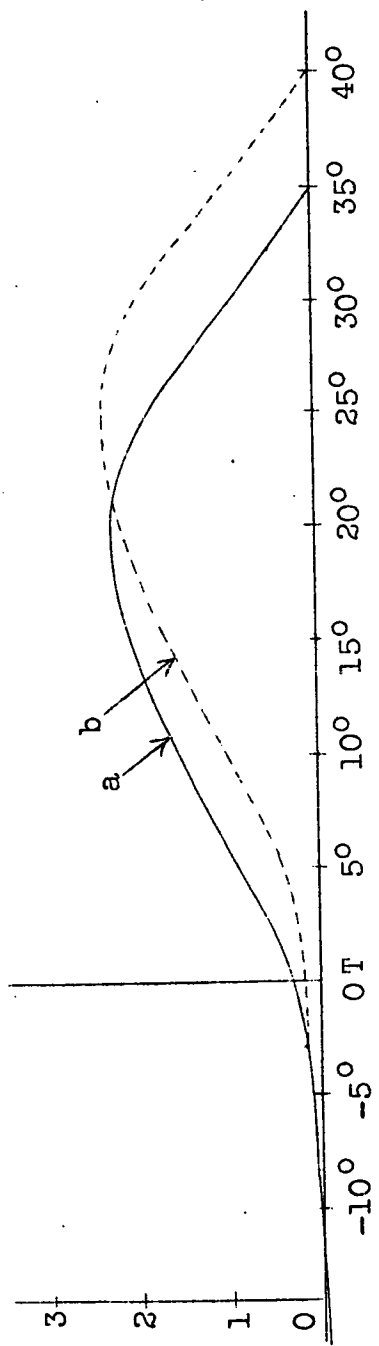


Fig.16

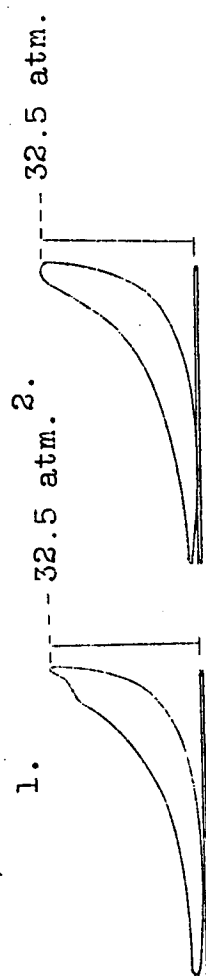


Fig.17

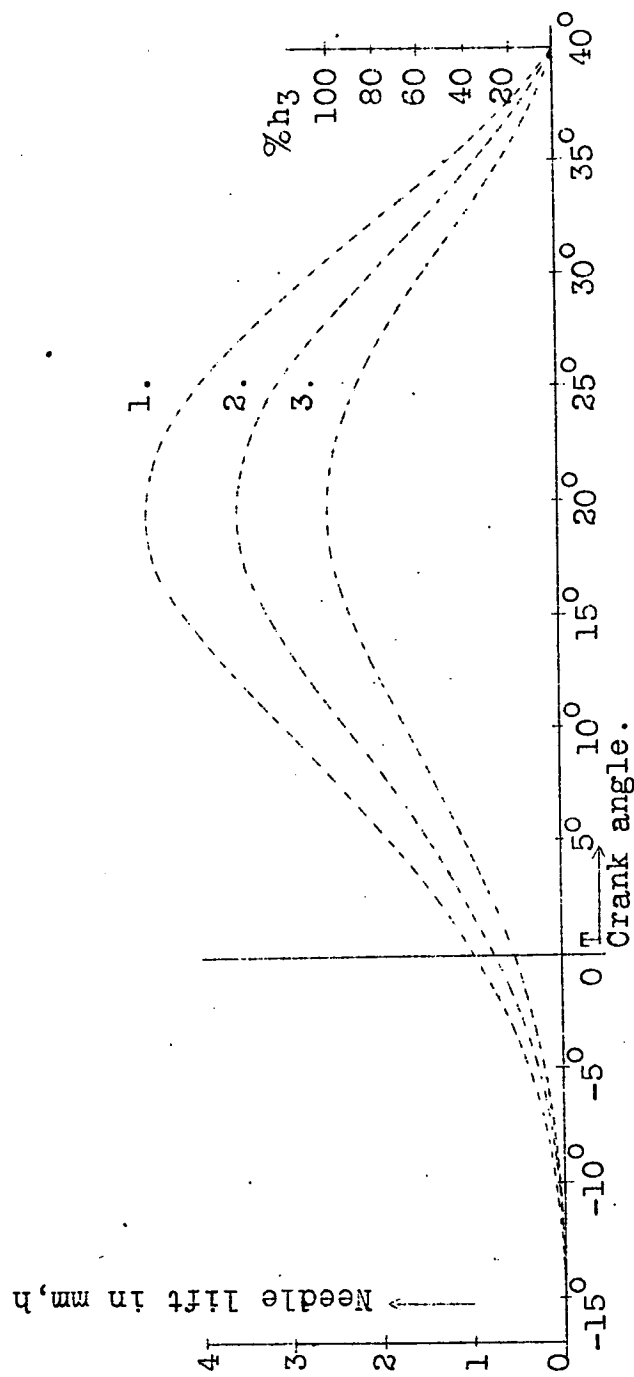


Fig.18

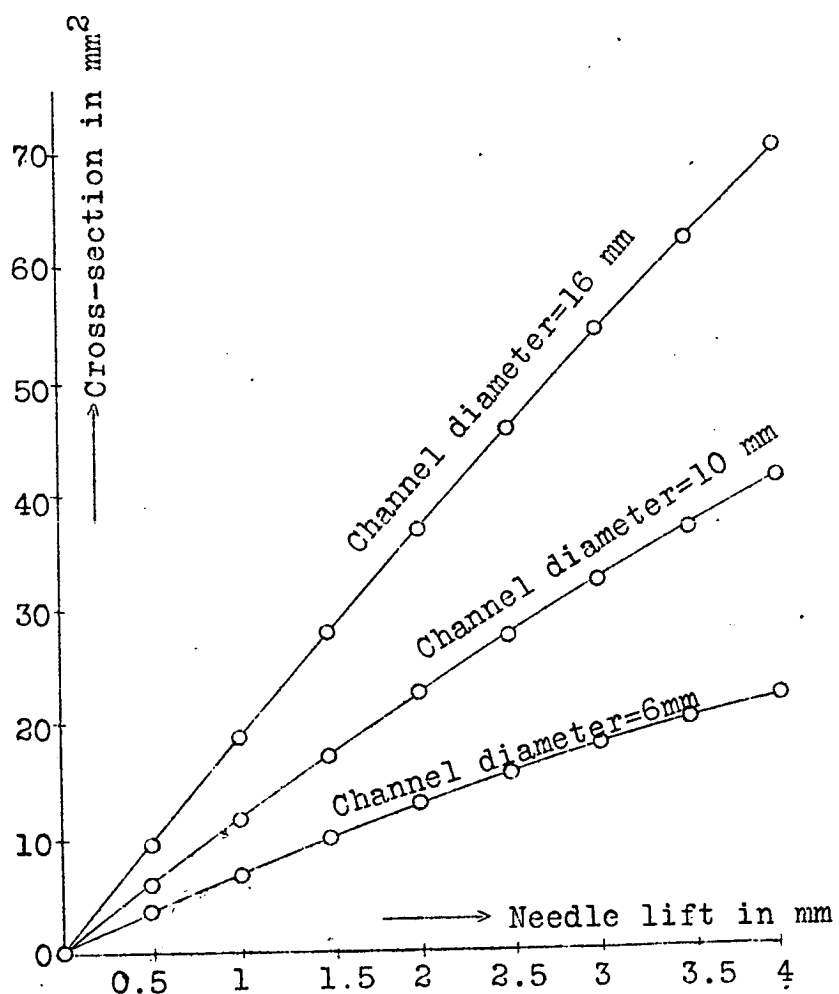


Fig.19 Cross-section curves.

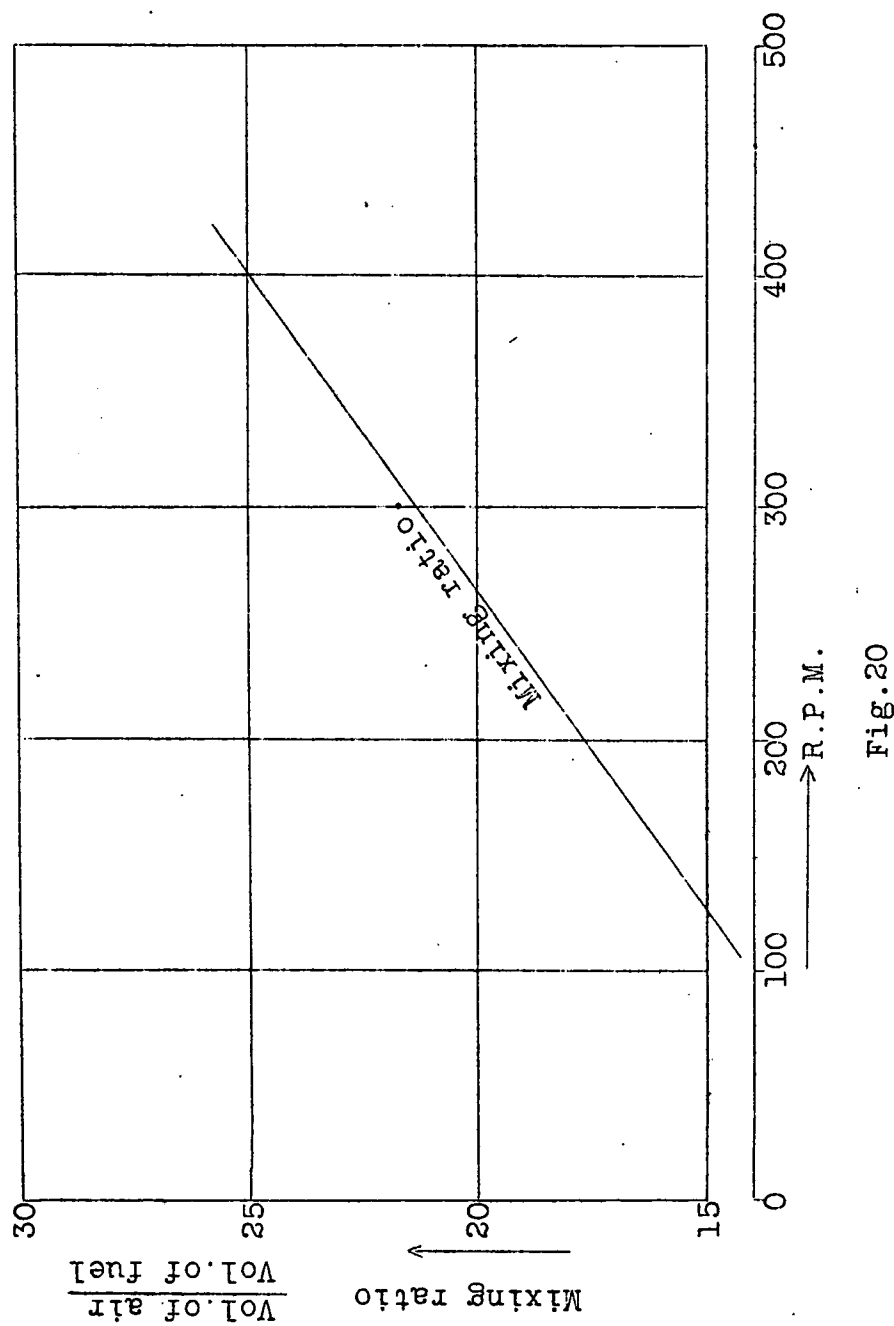


Fig.20

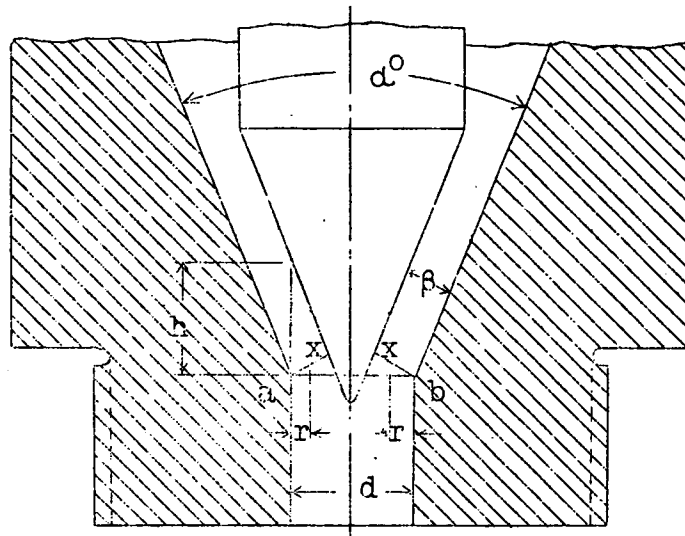


Fig.21

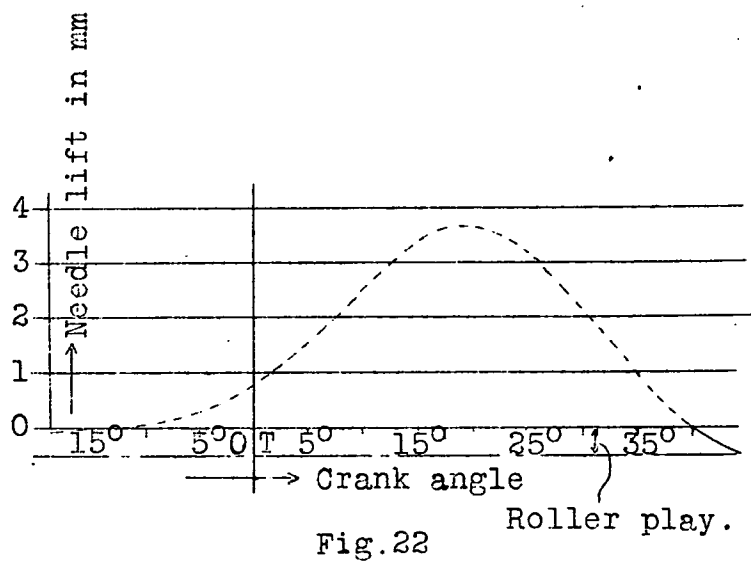


Fig.22